

Pentosan Polysulfate Maculopathy: Prevalence, Spectrum of Disease, and Choroidal Imaging Analysis Based on Prospective Screening



DERRICK WANG, SWETHA B. VELAGA, CHRISTELLE GRONDIN, ADRIAN AU, MUNESWAR NITTALA, JAY CHHABLANI, KIRAN K. VUPPARABOINA, FREDERIC GUNNEMANN, JOOYEON JUNG, JA-HONG KIM, MICHAEL IP, SRINIVAS SADDA, AND DAVID SARRAF

• **ABSTRACT:** Purpose: To describe the prevalence and spectrum of disease of pentosan polysulfate (PPS) maculopathy in a large multimodal retinal imaging study and to report the results of choroidal vascularity index (CVI) analysis.

Design: Prospective cohort study

Methods: Of 741 patients prescribed PPS within a large university database, 100 (13.4%) with any consumption agreed to participate in a prospective screening investigation. Multimodal retinal imaging including near-infrared reflectance (NIR), fundus autofluorescence (FAF), and spectral domain optical coherence tomography (SD-OCT) was performed in all patients. Characteristic findings of affected patients were identified, and affected and unaffected cohorts were compared. CVI, defined as stromal choroidal area (SCA) divided by the total choroidal area, was analyzed.

Results: The prevalence of PPS maculopathy was 16%. NIR illustrated punctate hyperreflective lesions with early presentation. FAF illustrated a speckled macular network of hypo- and hyperautofluorescence colocalized with multifocal hyperreflective retinal pigment epithelial lesions on SD-OCT. Advanced cases demonstrated varying degrees of atrophy. The affected cohort exhibited significantly greater mean PPS therapy duration, mean daily dosage, and mean cumulative dosage (19.5 ± 5.5 years, 433.9 ± 137.6 mg, $3,103.1 \pm 1,402.2$ g) compared with the unaffected cohort (7.1 ± 6.6 years, 291.6 ± 177.6 mg, 768.4 ± 754.8 g). SCA was significantly lower and CVI was significantly greater in the affected vs the unaffected group.

Conclusions: This prospective cohort study identified a prevalence of PPS maculopathy of 15%-20% among PPS users who agreed to participate. A spectrum of findings may be observed with multimodal retinal imaging. Significant choroidal abnormalities associated with this characteristic maculopathy may provide surrogate markers of macular toxicity. (Am J Ophthalmol 2021;227: 125–138. Published by Elsevier Inc.)

PENTOSAN POLYSULFATE SODIUM (PPS) IS THE SOLE oral medication approved by the United States Food and Drug Administration for the treatment of interstitial cystitis.¹ PPS was FDA-approved in 1996¹; however, recent studies have shown that long-term exposure can be associated with a pigmentary maculopathy.²

Although investigations continue to provide insight into this remarkable condition,³⁻⁷ much is still to be learned regarding PPS-associated retinal toxicity. Most of the current literature regarding the imaging features is based on retrospective studies instead of prospective analyses, and there is scarce information regarding the prevalence of this condition in the population of PPS users. Our group initially prospectively screened 50 patients ascertained from the UCLA database of PPS users and noted a prevalence of approximately 20%. Vora and colleagues⁴ screened PPS patients with a cumulative dosage of at least 500 g and found a prevalence of toxicity of 23%. Our initial study demonstrated that the risk of toxicity was greatest in PPS users with a cumulative dosage of greater than 1,000 g and especially greater than 1,500 g. Our group has since doubled the number of screened PPS patients at UCLA and additionally performed formal choroidal imaging analysis in the total cohort of screened subjects.

This study aimed to describe the prevalence and spectrum of disease of PPS maculopathy from our total cohort of PPS-treated patients at UCLA that were prospectively screened with multimodal retinal imaging analysis and to report the results of choroidal vascularity index (CVI) analysis.

Accepted for publication February 20, 2021.

Retinal Disorders and Ophthalmic Genetics, Stein Eye Institute, University of California Los Angeles (D.W., C.G., A.A., F.G., J.Y.J., D.S.), Los Angeles, California, USA; Doheny Image Reading Center, Doheny Eye Institute (S.B.V., M.N., M.I., S.V.S.), Los Angeles, California, USA; Department of Ophthalmology, UPMC Eye Center, University of Pittsburgh (J.C., K.K.V.), Pittsburgh, Pennsylvania, USA; Department of Urology, UCLA Medical Center, David Geffen School of Medicine at UCLA (J.H.K.), Los Angeles, California, USA; Department of Ophthalmology, David Geffen School of Medicine at University of California Los Angeles (M.I., S.V.S.), Los Angeles, California, USA; Greater Los Angeles VA Healthcare Center (D.S.), Los Angeles, California, USA

Inquiries to David Sarraf, Stein Eye Institute, University of California, Los Angeles, 100 Stein Plaza, Los Angeles, CA 90095, USA; e-mail: dsarraf@ucla.edu

METHODS

The University of California Los Angeles (UCLA) Institutional Review Board approved this cross-sectional study, which was conducted in accordance with the tenets set forth by the Declaration of Helsinki. Information was collected and secured in compliance with the Health Insurance Portability and Accountability Act. All data were deidentified and stored securely within the Stein Eye Institute.

A list of all patients prescribed PPS between the months of March 2013 and October 2019 from the UCLA electronic medical record was procured. The following key terms were used for the database search: *Elmiron 100mg PO caps*, *Elmiron PO*, *pentosan polysulfate sodium 100mg PO caps*, *pentosan polysulfate sodium PO*, and *pentosan polysulfate sodium POWD*. The search yielded 741 total UCLA patients treated with PPS arranged by date of first prescription. All 741 patients were contacted by telephone to request their participation in this study. After verbally confirming any history of PPS use, 100 patients (13%) consented to be participants. The other 641 patients who declined cited various reasons for not participating, including lack of interest, logistic limitations such as distance, out-of-state travel, or lack of transportation, and time constraints including inability to arrange visits into their schedule.

Patients were all (except for 2) prospectively screened with multimodal retinal imaging in the retina clinic. The participants first completed a questionnaire that included demographic information—date of birth, gender, identified race, height, and weight. Every participant's body mass index (BMI) was calculated via the National Heart, Lung, and Blood Institute online calculator on the basis of weight (pounds) and height (feet and inches). The questionnaire also asked about previous medical and ocular history, smoking history, PPS history (duration, daily dosage, any regimen changes during use), and development of visual symptoms while being treated with PPS.

All 100 patients underwent Snellen visual acuity testing and were screened with a series of multimodal retinal imaging studies that included 30- and 50-degree fundus autofluorescence (FAF) of the macula (Spectralis; Heidelberg Engineering Inc, Heidelberg, Germany), multicolor and near-infrared reflectance (NIR) of the macula (Spectralis; Heidelberg Engineering Inc), ultra-widefield autofluorescence of the posterior pole and periphery (Optos California *icg*; Optos Inc, Dunfermline, Scotland, UK), and color fundus photography of the posterior pole and periphery (Optos California *icg*; Optos Inc). Spectral domain optical coherence tomography (SD-OCT) (Spectralis; Heidelberg Engineering Inc) of the macula was also performed in all 100 patients and included a volume analysis of 25 B-scans (30 degrees by 20 degrees, B-scans spaced 240 μm apart).

OCT angiography (OCTA) and en face OCT (Solix; Optovue Inc, Fremont, California, USA) imaging were per-

formed only in affected patients and used the automated default segmentation at the levels of the superficial and deep retinal capillary plexuses and choriocapillaris.

Fundus photography, SD-OCT, and FAF imaging was already performed on patients 21 and 22 under the guidance of their retinal specialist at UCLA at the time of initial communication during the screening process; thus, imaging was not repeated.

To identify structural associations of the autofluorescence, FAF images were colocalized with en face OCT images. The segmentation for analysis of en face OCT was set to the retinal pigment epithelium. The upper limit of the segmentation band was set at the retinal pigment epithelial and ellipsoid zone junction; the lower limit was set at the retinal pigment epithelial and Bruch membrane junction. En face OCT slab thickness was 20 μm .

Atrophy noted with FAF and OCT were defined by criteria previously published in the literature.⁸⁻¹¹ The criteria for complete retinal pigment epithelial and outer retinal atrophy (cRORA) includes a continuous band of hypertransmission at least 250 μm in diameter, a continuous zone of retinal pigment epithelial attenuation or disruption at least 250 μm in diameter, and superimposed photoreceptor degeneration.^{8,9} Atrophy noted on FAF was defined as a well-demarcated round zone of hypoautofluorescence of nonspecific diameter.^{10,11}

The presence or absence of cRORA with OCT and atrophy with FAF were the basis for grading PPS-associated maculopathy severity in affected patients. This grading system was modified according to the original system previously published and was defined as follows³:

Mild PPS-associated maculopathy: Presence of a speckled pattern of hypo- and hyperautofluorescence on FAF (or only hyperautofluorescent lesions) and no evidence of well-demarcated atrophic lesions on FAF and no evidence of cRORA with SD-OCT.

Moderate PPS-associated maculopathy: Presence of well-demarcated, nummular, hypoautofluorescent atrophic lesions on FAF that colocalized with cRORA on SD-OCT within the macula but without central foveal involvement.

Severe PPS-associated maculopathy: Presence of hypoautofluorescent atrophy within the macula with colocalization with cRORA with SD-OCT and involving the central fovea.

An expert evaluator (D.S.) examined the multimodal imaging of all 100 patients to confirm the presence or absence of findings consistent with PPS-associated maculopathy based on those described in the literature.^{2,3,6}

Statistical analyses were performed using Prism 8 for macOS. Patient demographics, BMI, therapy duration, and daily and cumulative doses were reported as medians, means, and standard deviations (interval variables). Retinal findings on multimodal imaging were reported as numerical counts and percentages (ordinal variables).

Prevalence was calculated as number of affected individuals divided by total number of screened individuals. Snellen visual acuity was converted to logarithm of the minimum angle of resolution (logMAR) for statistical analysis, and mean logMAR was converted back to mean Snellen visual acuity as reported in the Results. The right eye was chosen arbitrarily for the comparison of visual acuity. χ^2 tests were used for sex and tobacco use (nominal variables). Wilcoxon signed-rank test was performed to compare the means of age, height, weight, BMI, visual acuity, duration of PPS intake, daily PPS dose, and cumulative PPS dose (nonparametric interval variables). $P < .05$ was considered statistically significant.

It is important to note that 10 of the 16 affected cases and the first 50 of the 100 total screened patients in this study were originally described in a prior published paper.³

• **CHOROIDAL VASCULARITY INDEX ANALYSIS:** For choroidal imaging analysis, raw OCT B-scans were analyzed using a MATLAB-based CVI quantification tool developed based on previously described image-processing methods.¹²⁻¹⁴ In brief, luminal choroidal area (LCA) and stromal choroidal area (SCA) were obtained by binarizing the choroid layer in the OCT B-scan, where dark pixels correspond to the luminal region and bright pixels correspond to the stromal region. To this end, a 2-pronged approach was adopted: (i) automated detection of the choroid layer using structural similarity index and tensor voting and (ii) automated binarization of the choroid layer based on exponential and nonlinear enhancement and median thresholding using the Otsu Technique. Shadow compensation, the process of making up for shadows that may influence visualization of posterior structures on OCT, was performed using the previously reported method.¹⁵ Finally, CVI (%) was calculated as the ratio of LCA to the total choroidal area (TCA) in both study cohorts. Subfoveal choroidal thickness (SFCT) was measured from the inner choroid boundary to the outer choroid boundary using the instrument calipers tool at the foveal center.

RESULTS

• **DEMOGRAPHICS AND DESCRIPTION OF THE TOTAL COHORT:** A total of 100 patients (200 eyes) that reported any previous history and/or current use of PPS irrespective of duration were screened for signs of retinal toxicity (Table 1). Of the 100, 97 were included in the final analysis cohort, because 3 cases based on image findings were deemed indeterminate (refer below to “Demographics and Description of the Indeterminate Cohort”). Median age of the entire cohort was 60 years (range: 23-93 years) and 89 of 97 (92%) were female. A total of 78 (80%) patients were non-Hispanic white whereas 2 (2%) patients were biracial. Mean weight and height were 144.4 ± 33.8

pounds and 64.7 ± 3.1 inches respectively. Mean BMI was 24.2 ± 5.0 . The mean visual acuity of the entire cohort was 20/25.

The overwhelming majority of patients (92/97, 95%) indicated that interstitial cystitis was the reason for using PPS. The other indications included irritable bowel syndrome, pelvic pain syndrome, inner bladder wall cracks, medical accident, and bladder pain, all of which were reported by nonaffected patients. No kidney or liver abnormalities were reported in any patients.

Mean total duration of PPS use was 9.2 ± 7.9 years, mean daily dose of PPS was 315.0 ± 179.0 mg, and mean cumulative dose of PPS was $1,153.5 \pm 1,241.2$ g (Table 1). The recommended dosage of PPS is 300 mg/d.¹⁶

• **DEMOGRAPHICS AND DESCRIPTION OF THE AFFECTED COHORT (COMPARED WITH THE NONAFFECTED COHORT):** Of the 97 patients, PPS-associated maculopathy was definitively identified in 16 (32 eyes), yielding a prevalence of approximately 16% (16/97), whereas 81 patients (162 eyes) failed to display any evidence of PPS maculopathy. Median age of the affected cohort was 64.5 years (range: 41-76 years). Of the 16 affected, 15 (94%) were female and 15 (94%) identified as non-Hispanic white.

The most common visual complaint in the affected cohort was nyctalopia ($n = 10$, 63%) followed by blurry vision ($n = 6$, 38%). Other symptoms included complaints of distortion by 2 patients and dulling of colors by 1 patient. Two affected patients were asymptomatic. Median Snellen visual acuity was 20/27.5 OD (range: 20/20–hand motion) and 20/27.5 OS (range: 20/20–20/400) in the affected cohort. Median IOPs were 15 mm Hg OD (range: 11-19) and 14.5 mm Hg OS (range: 9-22).

With slit lamp examination, 6 patients presented with varying forms of bilateral cataracts whereas 1 patient was pseudophakic OD with a cataract OS. One patient was noted to have asteroid hyalosis. The remaining 8 patients exhibited normal bilateral anterior segment examinations. Within the cataract group, a nasal conjunctival hemorrhage OD was noted in one patient and Krukenberg spindles OU were noted in another. On fundus examination, 8 patients and 16 eyes (16/32, 50%) displayed only bilateral pigmentary maculopathy of varying degrees. One patient and 2 eyes (2/32, 6%) displayed only bilateral retinal pigment epithelial atrophy. Five patients (10/32 eyes, 31%) displayed a combination of bilateral retinal pigment epithelial atrophy and pigmentary maculopathy to varying degrees. Normal macular examination was noted in 2 affected patients (4/32 eyes, 13%). Heme or fluid was not identified in any affected eyes.

Affected and unaffected groups were compared (Table 1). No statistically significant difference was found between the 2 groups in terms of age, sex, smoking history, height, weight, or BMI. However, the affected group exhibited a significantly longer duration of PPS use, higher daily dosage, and greater cumulative dose compared with the

TABLE 1. Demographics, Dosage Parameters, and Visual Acuity of Total Cohort Excluding Indeterminate Cohort, and Unaffected and Affected Groups

	Total (n=97)	Unaffected (n=81)	Affected (N=16)	P value
Age, mean ± SD (median)	57.4±15.5 (60)	56.5±16 (59)	62±11.9 (64.5)	.19
Sex, n (%)				1.0
Male	8 (8.2)	7 (8.6)	1 (6.3)	
Female	89 (91.8)	74 (91.4)	15 (93.7)	
Tobacco users, n (%)	23 (23.7)	20 (24.7)	3 (18.8)	1.0
Height, in., mean ± SD (median)	64.7±3.1 (64)	65.8±8.7 (65)	63.6±3.4 (63.3)	.32
Weight, lb, mean ± SD (median)	144.4±33.8 (140)	145.9±33.5 (141)	136.6±35.8 (131.5)	.31
BMI, mean ± SD (median)	24.2±5.0 (23.1)	24.3±4.9 (23.6)	23.6±5.4 (22.4)	.61
Visual acuity, logMAR, mean ± SD (median Snellen equivalent)	0.1±0.3 (20/20)	0.05±0.2 (20/20)	0.3±0.6 (20/27.4)	.0003
Duration of PPS intake, y, mean ± SD (median)	9.2±7.9 (7)	7.1±6.6 (5)	19.5±5.5 (18)	<.0001
Daily PPS dose, mg, mean ± SD (median)	315.0±179.0 (300)	291.6±177.6 (300)	433.9±137.6 (400)	.0032
Cumulative PPS dose, g, mean ± SD (median, range)	1,153.5±1,241.2 (703, 12.2-6,023)	768.4±754.8 (493, 12.2-3,103)	3,103.1±1,402.2 (2,737.5, 1,533-6,023)	<.0001

logMAR = logarithm of the minimum angle of resolution, PPS = pentosan polysulfate sodium.

unaffected group. The mean duration of PPS intake was 19.5±5.5 years (median: 18 years, $P < .0001$) in the affected group vs 7.1±6.6 years (median: 5 years) in the unaffected group. The affected cohort reported a higher mean daily dose of 433.9±137.6 mg (median: 400 mg, $P = .0032$) vs 291.6±177.6 mg (median: 300 mg) in the normal group. The affected group also reported a greater mean cumulative dose of 3,103.1±1,402.2 g (median: 2,737.5 g, $P < .0001$) vs 768.4±754.8 g (median: 493 g) in the nonaffected group. Additionally, the affected cohort exhibited significantly worse visual acuity (mean Snellen visual acuity 20/43 vs 20/22, P value = .0003).

There was overlap in the ranges of cumulative dose between the affected and unaffected groups. The minimum cumulative dose at which PPS retinal toxicity was definitively found was 1,533 g. Of note, 12 patients (12/81, 15%) of the unaffected cohort reported higher cumulative doses: patient 3 (2,336 g), patient 6 (3,103 g), patient 15 (1,643 g), patient 46 (1,889 g), patient 50 (1,898 g), patient 52 (2,701 g), patient 65 (2,737.5 g), patient 71 (2,299.5 g), patient 76 (2,920 g), patient 85 (1,861.5 g), patient 86 (1,971 g), and patient 98 (1,837 g). The prevalence of toxicity in those with cumulative dosages greater than 1,000 and 1,500 g was 40% and 55%, respectively.

• **MULTIMODAL RETINAL IMAGING FINDINGS OF THE AFFECTED COHORT:** Since the initial studies that first described PPS maculopathy, wide-field FAF and SD-OCT have been proposed to be the optimal combination to detect the characteristic macular alterations stemming from long-term PPS exposure (Figure 1).^{2,3,6} NIR and multicolor imaging can also effectively identify PPS maculopathy alterations especially in the mildest affected cases.³

In the 16 affected patients, the severity and total area of abnormal autofluorescence varied across a wide spectrum. FAF was remarkable for well-circumscribed regions of the typical speckled pattern of hyper- and hypoautofluorescence surrounding the fovea and spreading outward to varying degrees (Figure 1) in 26 eyes out of 32 (81%). The network of hyper- and hypoautofluorescence extended around the disc in 17 eyes out of these 26 (65%). Of note, peripapillary atrophic hypoautofluorescent rings were noted in 100% (32/32) of affected eyes. In 6 eyes (19%), FAF was remarkable for more atypical patterns. FAF in patient 47 (Figure 2) was remarkable for an extremely subtle speckled parafoveal hyperautofluorescence. FAF in patient 18 showed parafoveal hyperautofluorescent vitelliform-like deposits bilaterally. FAF in patient 100 showed a hyperautofluorescent patternlike abnormality in the right eye (robust genetic testing was performed and a pattern dystrophy due to a PRPH2 mutation was excluded) and a hyperautofluorescent acquired vitelliform lesion central in the left eye.

More severe forms of disease (consistent with a moderate grade of PPS maculopathy) with atrophy were noted in 7 eyes (25%) out of 32. These eyes illustrated atrophy in the form of parafoveal nummular lesions of hypoautofluorescence. These atrophic areas ranged from smaller than one-disc diameter to larger than one-disc diameter or diffuse atrophy. Bilateral diffuse areas of geographic atrophy involving the central fovea (consistent with a severe grade of PPS maculopathy) were present in 4 eyes out of 32 (cases 51 and 21). Atrophy was also noted in the periphery in patient 21.

SD-OCT imaging was remarkable for discrete focal areas of hyperreflective retinal pigment epithelial thickening that colocalized with the hyperautofluorescent alterations

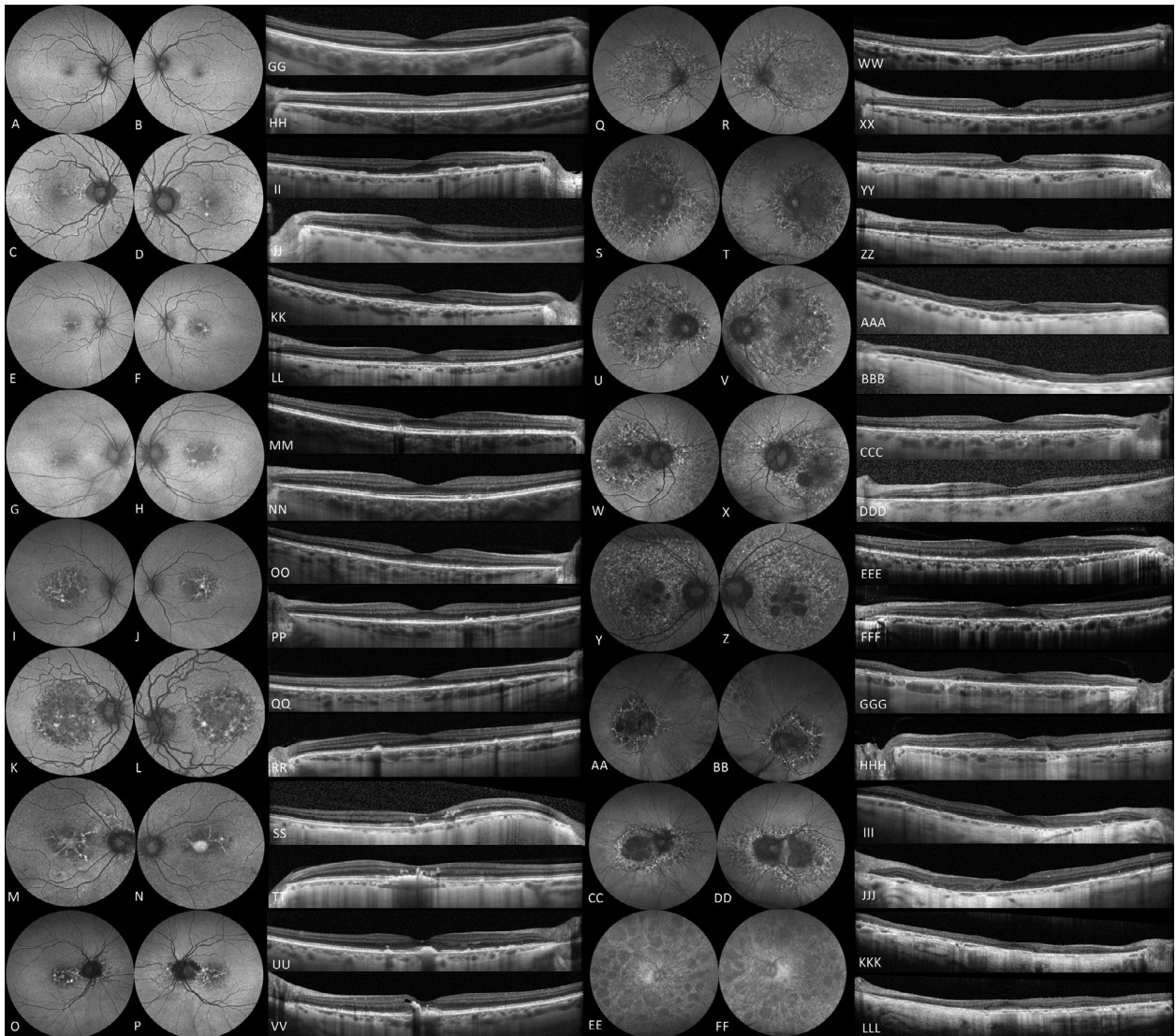


FIGURE 1. Fundus autofluorescence images (FAF, A-FF) and spectral domain optical coherence tomography (SD-OCT) B-scans through the fovea (GG-LLL) of all affected patients with pentosan polysulfate maculopathy. Note the wide range of findings identified with FAF. The mildest presentation (A&B, patient 47) is remarkable for FAF that illustrates subtle perifoveal hyperautofluorescent lesions in each eye. The near-infrared reflectance (NIR) and multicolor images were more conclusive in this case. The SD-OCT B-scan shows a small corresponding hyperreflective retinal pigment epithelium lesion OS. FAF and NIR for patient 18 (C&D, II&JJ) illustrate hyperautofluorescent and hyperreflective vitelliform-like lesions. More advanced toxicity is illustrated with patients 57, 88, 58, and 10 (E&F through K&L) in whom a speckled pattern of hyper- and hypoautofluorescent lesions with FAF and hyperreflective retinal pigment epithelial lesions with SD-OCT, of progressive severity, are noted only in the macula. With more advanced toxicity, the speckled pattern extends around and nasal to the disc and into the periphery (M&N through S&T, patients 100, 43, 95, and 34, respectively). Defined areas of nummular and geographic hypoautofluorescent atrophy of the retinal pigment epithelium are noted with more severe toxicity (U&V to EE&FF, patients 39, 29, 22, 44, 51, and 21). The OCT B-scans exhibit areas of corresponding complete retinal pigment epithelial and outer retinal atrophy. The most severe case (EE&FF, patient 21) is remarkable for diffuse chorioretinal atrophy of the posterior pole and periphery. The hypoautofluorescent atrophy on FAF corresponds to diffuse retinal pigment epithelial and outer retinal atrophy on SD-OCT. Of note, all 32 affected eyes illustrated halos of peripapillary hypoautofluorescent atrophy.

noted with FAF (Figure 1). Of note, the hypoautofluorescent areas on FAF constituting the typical speckled pattern did not correspond with any outer retinal or retinal pigment epithelial abnormalities on OCT; however, the darker well-

demarcated nummular hypoautofluorescent lesions in cases of greater severity colocalized with cRORA.

Multicolor and NIR illustrated bright orange and hyperreflective punctate lesions respectively, corresponding to

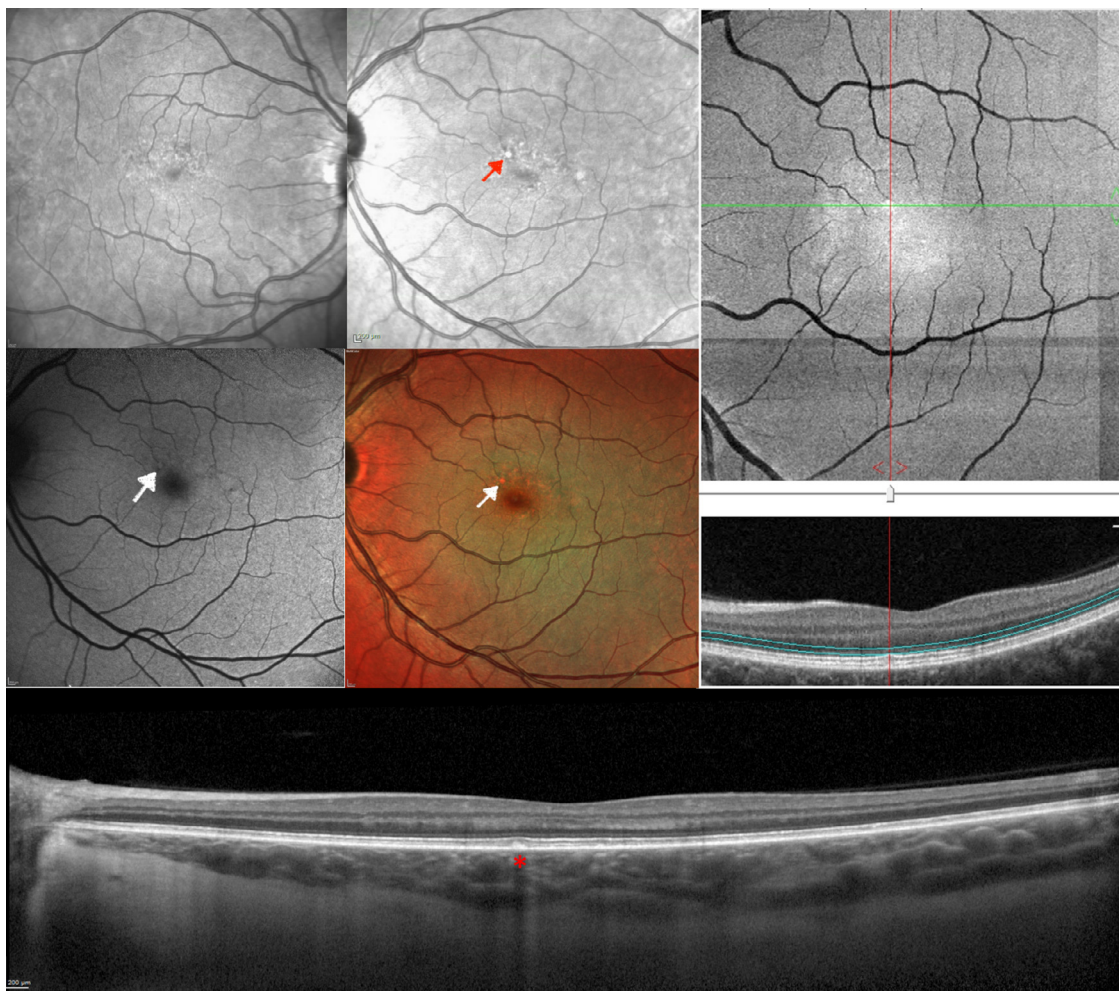


FIGURE 2. Near-infrared reflectance (NIR) of both eyes and fundus autofluorescence (FAF), multicolor (MC), en face optical coherence tomography (OCT), and spectral domain optical coherence tomography (SD-OCT) of the left eye from the mildest case (patient 47) of the affected cohort. NIR (top row left and middle) reveals abnormal pentosan polysulfate (PPS)-related hyperreflective dots. The arrows in the NIR, FAF (middle row left), and MC (middle row middle) identify the most prominent hyperreflective lesion indicating very early evidence of PPS maculopathy. The lesion appears hyperreflective on en face OCT (right) and colocalizes with retinal pigment epithelial thickening noted on SD-OCT (bottom) as identified with the red asterisk.

hyperautofluorescent lesions on FAF and focal retinal pigment epithelial thickening on OCT in the mild cohort. Multicolor and NIR were more revealing than FAF and OCT in patients 47 (Figure 2) and 18, the 2 mildest cases of the affected cohort. In cases of greater severity, atrophic regions showed increased visualization of the underlying choroid.

Color fundus photography displayed pigment deposits that colocalized with the FAF hyperautofluorescent lesions and the areas of multifocal hyperreflective retinal pigment epithelial thickening with SD-OCT. En face OCTA showed reduced perfusion in the choriocapillaris aligned with the cRORA lesions; the other segmentation levels were normally perfused.

Choroidal neovascularization was identified in the right eye of 1 affected patient (patient 95). Choroidal neovascu-

larization associated with PPS maculopathy has been previously described.¹⁷

- **SEVERITY GRADING IN THE AFFECTED COHORT:** The 16 affected patients were classified into 3 categories (mild, moderate, severe) based on the presence or absence of atrophy and the extent of atrophy, as defined in the Methods section, using FAF and OCT guidance. Patients 47 (Figure 2), 18, 57, 88, 58, 10, 100, 43, 95, and 34, listed in order of increasing severity, exhibited mild-grade PPS maculopathy in each eye (ie, total of 20 eyes in this cohort with mild maculopathy) and failed to show any signs of atrophic hypoautofluorescence on FAF or cRORA on SD-OCT. Patients 39, 29, 22 (Figure 3), and 44, listed in order of increasing severity, exhibited a moderate-grade maculopathy (ie, total of 7 eyes with moderate maculopathy, 1

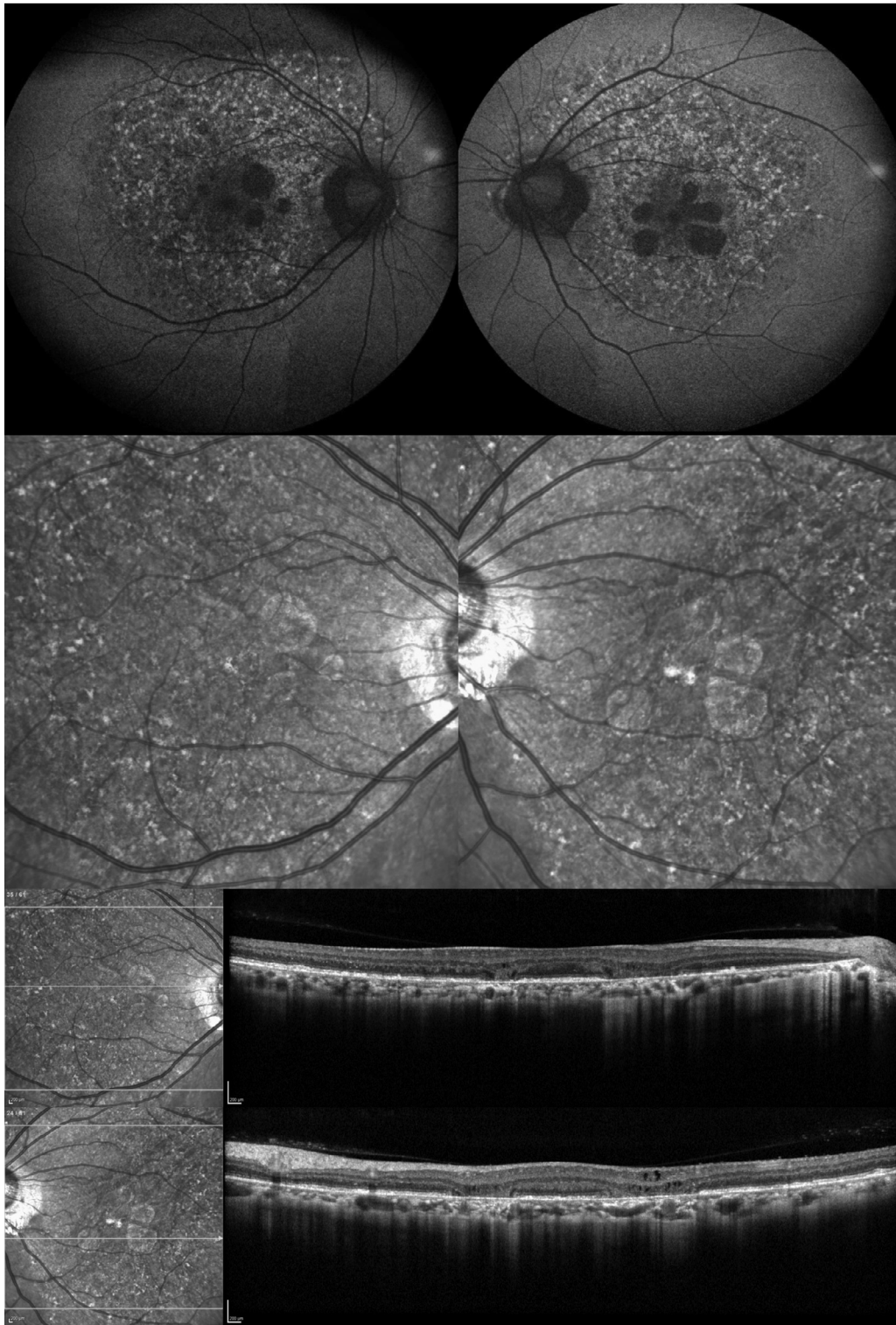


FIGURE 3. Moderate severity grade of pentosan polysulfate (PPS) maculopathy as illustrated with fundus autofluorescence (FAF), near-infrared reflectance (NIR), and spectral domain optical coherence tomography (SD-OCT) in patient 22. FAF (top row) illustrates nummular areas of parafoveal hypoautofluorescence representing atrophy distributed within the characteristic speckled pattern of autofluorescence classic for PPS maculopathy. NIR (second row) displays hyperreflective punctate lesions corresponding to the typical hyperautofluorescent FAF lesions of PPS toxicity and associated nummular or geographic atrophy. The selected SD-OCT B-scans (bottom 2) from each eye show corresponding areas of complete retinal pigment epithelial and outer retinal atrophy (cRORA) that colocalize with the pericentral areas of atrophy on FAF.

TABLE 2. Comparison of Dosage Parameters Between Patients With Varying Severity of Disease

	Mild (n=10)	Moderate (n=4)	Severe (n=2)
Duration of PPS intake, y, median (range)	18.0 (12.5-29.0)	19.2 (12.0-30.0)	22.3 (17.0-27.5)
Mean daily PPS dose, mg, median (range)	400.0 (200.0-629.0)	325.0 (300.0-593.8)	588.2 (576.5-600.0)
Cumulative PPS dose, g, median (range)	2,518.5 (1,752.0-5,402.0)	2,646.3 (1,533.0-4,334.0)	4,800.0 (3,577.0-6,023.0)

PPS = pentosan polysulfate sodium.

eye of patient 39 was mild) with nummular atrophic lesions and cRORA with FAF and OCT, respectively, limited to the macula around the fovea. Patients 51 (Figure 4) and 21, listed in order of increasing severity, exhibited severe grade of PPS maculopathy in each eye (ie, total of 4 eyes with severe maculopathy) with diffuse atrophy (including geographic hypoautofluorescence with FAF and cRORA with SD-OCT) in the macula that extended through the central fovea.

All cases of PPS toxicity were bilateral, including the mildest case in which only very subtle lesions were present in each eye. Severity grading of toxicity was identical bilaterally in all patients except for patient 39 (moderate OD and mild OS; U&V and AAA&BBB in Figure 1), and findings were remarkably symmetrical in all subjects, although not necessarily identical, in one eye vs the other in terms of the location, features, and extent of pathologic findings (Figure 1).

Table 2 compares the duration of PPS intake, mean daily dose, and cumulative dose among the 3 severity classifications. Statistical comparisons could not be done because of small sample sizes. The severity of alterations corresponded with increasing duration of PPS intake and cumulative dose but not daily PPS dose. Median cumulative dosages were 2,518.5 g, 2,646.3 g, and 4,800 g in the mild, moderate, and severe groups, respectively. Of note, some of the higher cumulative doses were noted in patients with mild or moderate presentations. The median duration of PPS intake was 18 years, 19.2 years, and 22.3 years and the median daily PPS dose was 400 mg, 325 mg, and 588.2 mg in the mild, moderate, and severe cohorts, respectively. It is important to note, however, that the correlation between severity classification and duration of PPS therapy and cumulative exposure may be skewed by the most severe patient with the greatest cumulative exposure from a group of only 2 patients.

• **DEMOGRAPHICS AND DESCRIPTION OF THE INDETERMINATE COHORT:** Three patients (3/100, 3%) were classified as indeterminate cases because of either a coexisting ocular disorder or uncertainty regarding the diagnosis of PPS maculopathy. Median age of these 3 cases was 66 years (range: 64-70 years). All 3 were female and non-Hispanic white. Mean weight and height were 152.3±12.0 pounds and 62.3±0.6 inches, respectively. Mean BMI was

27.5±1.7. The mean visual acuity of this indeterminate cohort was 20/33. All 3 of these indeterminate patients reported PPS treatment for interstitial cystitis. No kidney or liver abnormalities were reported in these patients. Mean duration of PPS intake was 19.5±4.8 years, mean daily PPS dose was 233.3±57.7 mg, and mean cumulative PPS dose was 1,727.7±876.3 g.

• **MULTIMODAL RETINAL IMAGING FINDINGS OF THE INDETERMINATE COHORT:** Patient 77 (duration of PPS intake = 17.5 years, mean daily PPS dose = 200 mg, cumulative PPS dose = 1,277.5 g) presented with minimal findings. Hyper- and hypoautofluorescent abnormalities were not detectable on FAF. Subtle punctate hyperreflective lesions, suggestive of PPS toxicity, were noted around the fovea with NIR and en face OCT with very subtle corresponding retinal pigment epithelial alterations with SD-OCT.

In patient 79 (duration of PPS intake = 16 years, mean daily PPS dose = 200 mg, cumulative PPS dose = 1,168 g) (Figure 5), FAF was remarkable for central lesions resembling a pattern dystrophy with a hyperautofluorescent butterfly-like lesion in the central macula of each eye and corresponding hyperreflective lesions with NIR and retinal pigment epithelial thickening with SD-OCT, highly suggestive of PPS maculopathy. The surrounding hypoautofluorescent area colocalized with hypopigmentation on color fundus photography. Peripapillary atrophy was present in each eye. This patient refused genetic testing to exclude a pattern dystrophy.

Multimodal retinal imaging findings for patient 75 (duration of PPS intake = 25 years, mean daily PPS dose = 300 mg, cumulative PPS dose = 2,737.5 g) were remarkable for myopic degeneration with evidence of peripapillary atrophy with FAF and thin choroid with SD-OCT in each eye. FAF did display a subtle hyperautofluorescent speckled pattern around the central macula and disc in each eye, highly suspicious for PPS maculopathy.

• **CHOROIDAL ANALYSIS:** A total of 95 eyes, 26 affected (27%) and 69 unaffected (73%), out of a possible 200 eyes (48%) were analyzed for the different parameters of CVI (Table 3). The other 105 eyes were excluded because of inadequate image quality for analysis or for age-matching purposes. None of the indeterminate case eyes were included in the choroidal analysis. The 2 cohorts were age-matched with no significant difference in mean age (60.79±12.18

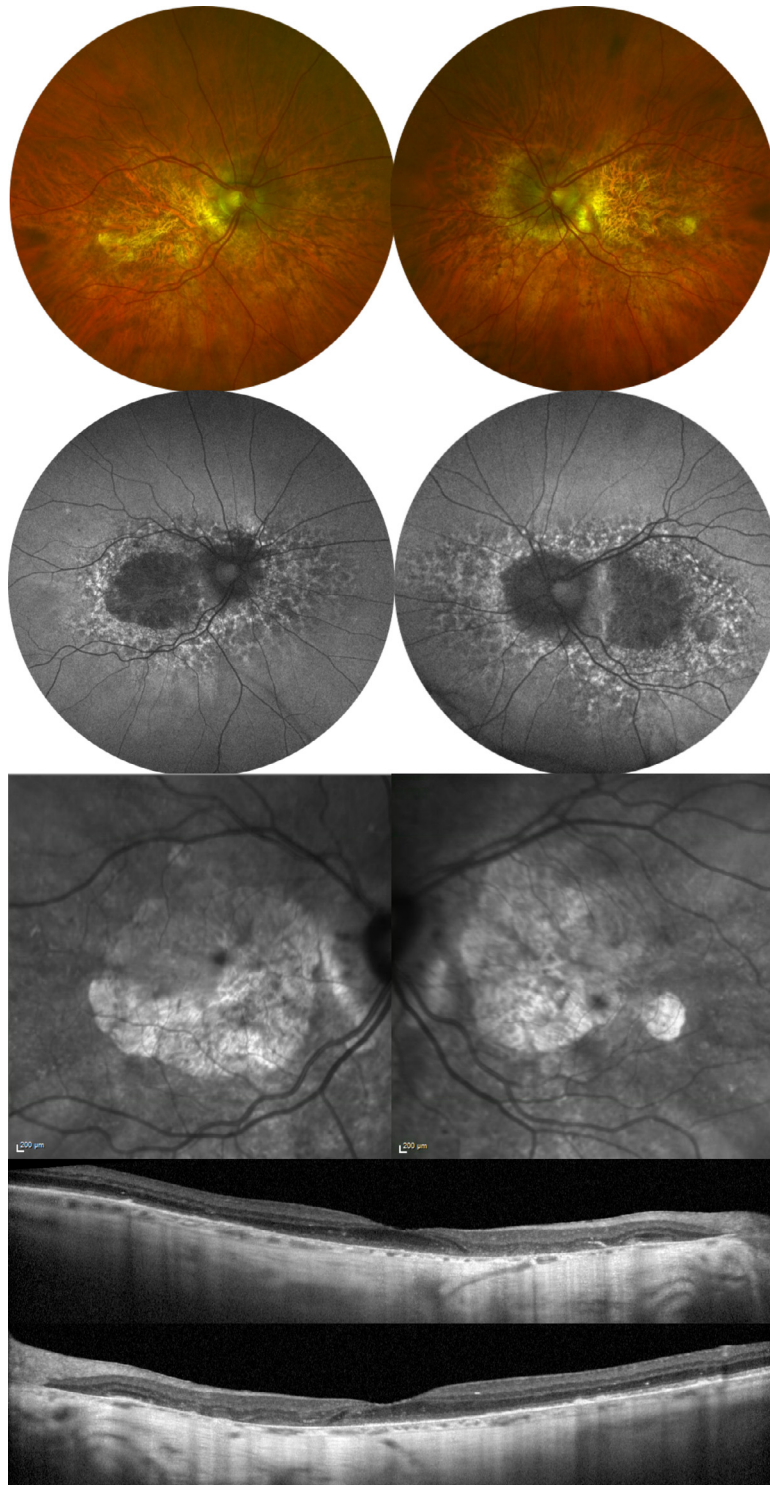


FIGURE 4. Severe grade of pentosan polysulfate maculopathy as illustrated with color fundus photography, fundus autofluorescence (FAF), near-infrared reflectance (NIR), and spectral domain optical coherence tomography (SD-OCT) in patient 51. Color fundus photography (top row), FAF (second row), and NIR (third row) illustrate a large area of geographic atrophy involving the central fovea corresponding to complete retinal pigment epithelial and outer retinal atrophy (cRORA) on SD-OCT (bottom row).

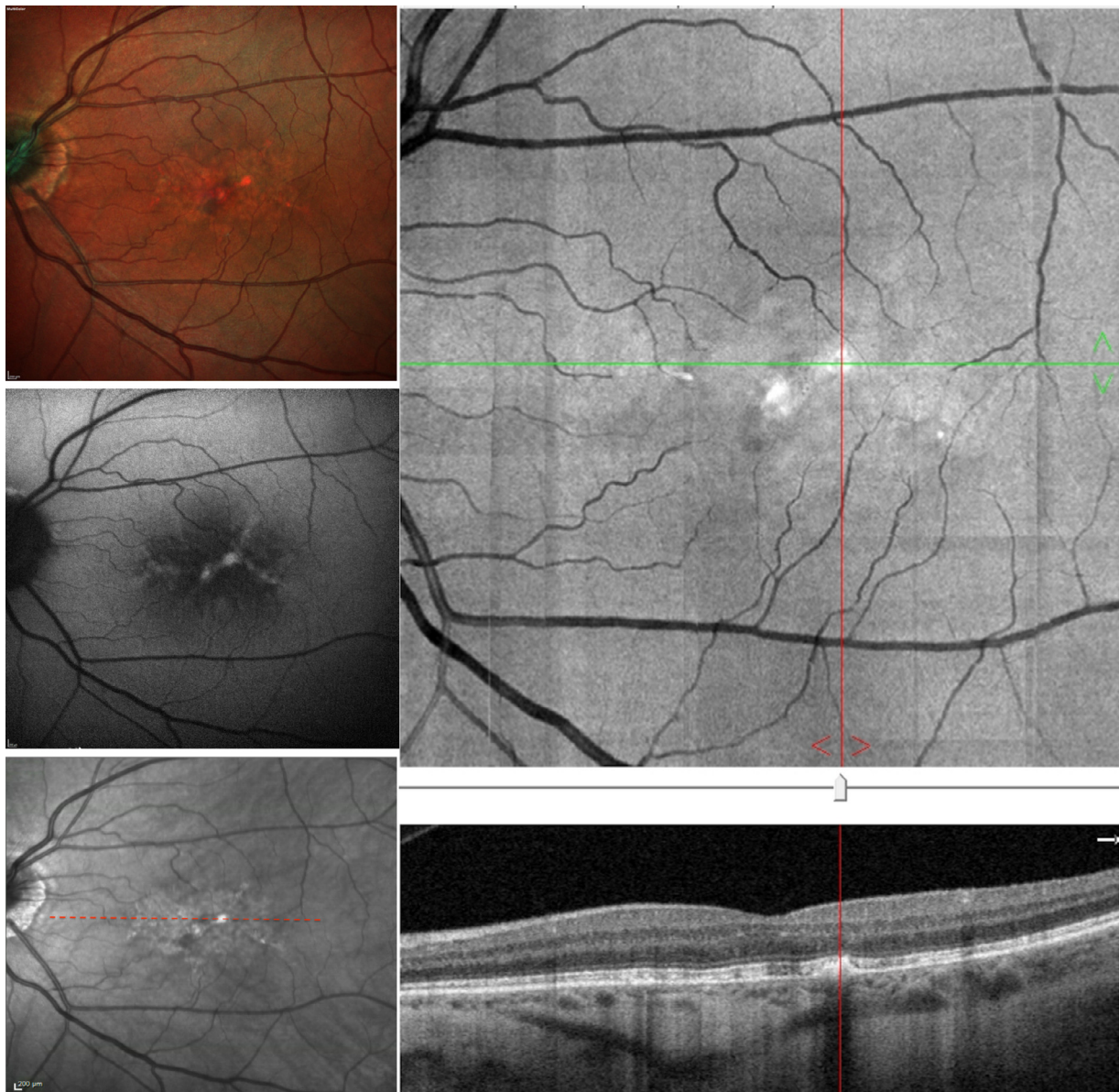


FIGURE 5. Multicolor (MC), fundus autofluorescence (FAF), near-infrared reflectance (NIR), and en face optical coherence tomography (OCT) of the left eye from indeterminate patient 79. With MC, FAF, and NIR (left side), a characteristic butterfly pattern dystrophy is illustrated. On en face OCT, these lesions appear as areas of hyperreflective retinal pigment epithelial thickening.

TABLE 3. Differences in Age and Choroidal Analysis Parameters Between Affected and Unaffected Cohorts

Parameters	Affected (n = 26 eyes)	Unaffected (n = 69 eyes)	P value	P ^a
Age, y, mean ± SD (range)	60.79 ± 12.18 (41-76)	63.14 ± 11.03 (38-77)	.51	
Total choroidal area, mm ² , mean ± SD (range)	0.29 ± 0.14 (0.11-0.58)	0.31 ± 0.18 (0.11-1.29)	.63	.61
Stromal area, mm ² , mean ± SD (range)	0.09 ± 0.04 (0.03-0.17)	0.11 ± 0.07 (0.03-0.54)	.04	.09
Luminal area, mm ² , mean ± SD (range)	0.20 ± 0.11 (0.08-0.44)	0.20 ± 0.11 (0.07-0.76)	.84	.88
Choroidal vascularity index, %, mean ± SD (range)	67.23 ± 5.07 (54-76)	63.11 ± 5.60 (48-74)	.001	.001
Subfoveal choroidal thickness, μm, mean ± SD (range)	238.42 ± 127.24 (94-487)	249.87 ± 89.59 (78-498)	.68	.24

^aControlled for intereye correlations using analysis of covariance.

TABLE 4. Differences in Age and Choroidal Analysis Parameters Between Mildly Affected and Unaffected Cohorts

Parameters	Affected (n = 17 eyes)	Unaffected (n = 69 eyes)	P value
Age, y, mean ± SD (range)	58.90 ± 11.30 (41-74)	63.14 ± 11.03 (38-77)	.29
Total choroidal area, mm ² , mean ± SD (range)	0.30 ± 0.13 (0.16-0.58)	0.31 ± 0.18 (0.11-1.29)	.75
Stromal area, mm ² , mean ± SD (range)	0.10 ± 0.03 (0.05-0.16)	0.11 ± 0.07 (0.03-0.54)	.04
Luminal area, mm ² , mean ± SD (range)	0.21 ± 0.11 (0.10-0.44)	0.20 ± 0.11 (0.07-0.76)	.75
Choroidal vascularity index, %, mean ± SD (range)	68.00 ± 5.00 (59-77)	63.11 ± 5.60 (48-74)	.004
Subfoveal choroidal thickness, μm, mean ± SD (range)	228.30 ± 113.64 (94-487)	249.87 ± 89.59 (78-498)	.4

years for affected vs 63.14±11.03 years for unaffected). In the affected group, mean TCA was 0.29±0.14 mm², mean SCA was 0.09±0.04 mm², and mean LCA was 0.20±0.11 mm². In the unaffected cohort, mean TCA was 0.31±0.18 mm², mean SCA was 0.11±0.07 mm², and mean LCA was 0.20±0.11 mm². Of the 3 area parameters, only SCA was significantly different (significantly lower in the affected cohort) with a *P* value of .04. CVI was highly significantly different (*P* value = .001) between the affected cohort (67.23%±5.07%) and the unaffected cohort (63.11%±5.60%). There was no significant difference between SFCT in the affected (238.42±127.24 μm) and unaffected (249.87±89.59 μm) groups.

The same CVI analysis was performed including only the mildly affected cohort with PPS maculopathy to minimize any skew caused by the most severe cases with atrophy. In this repeat analysis, SCA remained significantly lower and CVI remained significantly higher in the affected group (Table 4).

DISCUSSION

The classic presentation of PPS maculopathy has been well described and includes an FAF speckled pattern of hyper- and hypoautofluorescent lesions centered around the fovea and in many cases around the optic disc as well.^{2,3,6} These lesions correspond to nonspecific focal areas of hyperreflective retinal pigment epithelial thickening. However, this study has broadened the spectrum of associated findings and highlighted the importance of multimodal retinal imaging. Very mild cases of PPS-associated maculopathy may only display subtle perifoveal hyperreflective punctate lesions with NIR or multicolor analysis. Variable presentations include acquired vitelliform lesions or even pattern- or butterfly-like dystrophy with FAF. More advanced cases with moderate disease are notable for pericentral nummular areas of hypoautofluorescent atrophy on FAF that colocalize with cRORA on OCT. Severe cases can illustrate central geographic atrophy, diffuse macular atrophy, or diffuse atrophy extending to the periphery. We have refined our previously published grading scale for PPS maculopathy³ and have illustrated that a more advanced grade of retinopathy

in this analysis may correlate with greater PPS exposure and toxicity.

Recent reports have calculated a prevalence of PPS-related maculopathy in the range of 20%-23%.^{3,4} The prevalence of 16% in this study may be a more accurate representation (although this prevalence would be 19% if the 3 indeterminate cases were included) as this analysis prospectively screened a population of PPS users and employed uniform multimodal imaging analysis. In Vora and colleagues' study, only OCT and fundus photography were used to screen the study patients, whereas FAF and NIR were not available in many of the cases.⁴ OCT and fundus photography can identify nonspecific features of PPS maculopathy; however, FAF may be the most important modality to detect the characteristic PPS alterations in the macula^{2,6} and NIR is critical to detect mild grades of maculopathy.³ Although this study did prospectively screen a cohort of 100 PPS users from a population of close to 750 patients, the true prevalence of PPS maculopathy needs to be validated in even larger population studies that include thousands of patients.¹⁸

We recently recommended screening guidelines based on the report of our first 50 published patients. The present study, which approximately doubles the number of prospectively screened subjects, confirms our original recommendations. We recommend baseline examination of all patients starting treatment with PPS to include multimodal retinal imaging with FAF, NIR, and SD-OCT. Patients with cumulative dosages >500 g should receive annual multimodal imaging, and those with dosages >1,000 g, especially >1,500 g, should be vigilantly monitored for macular toxicity. In this study, the range of cumulative exposure in the definitively affected patients was 1,533-6,023 g. If the 3 ambiguous cases were included, the lower threshold of the range would decrease to 1,168 as 2 of these 3 patients reported cumulative dosages of 1,168 and 1,277.5 g. Although none of the affected or indeterminate cases reported cumulative dosages less than 1,000 g, we support our previous study's³ recommendation of annual SD-OCT, NIR, and FAF testing beginning at a cumulative dosage of 500 g given the findings of the study by Hanif and colleagues that reported an affected patient with possible macular toxicity below 500 g and 7 affected patients between 500 and 1,000 g.⁶ It is also important to note that

10%-20% of our affected cases were asymptomatic, emphasizing the importance of earlier preventive screening.

This is the first study to formally analyze the effects of PPS toxicity on the choroid. CVI is a well-established metric to separately assess the vascular and stromal components of the choroid. We have previously used this tool to study the choroid in various diseases such as central serous chorioretinopathy and retinitis pigmentosa complicated by cystoid macular edema.¹⁹ In this study, the SCA was found to be significantly lower in the affected cohort vs the non-affected cohort, and CVI was correspondingly significantly greater in the affected group. Therefore, it is inferred that the higher CVI may be attributed to alterations in the choroidal stromal tissue in PPS-affected patients whereas the choroidal vasculature may not show evidence of harm.

PPS can readily bind to epithelial tissues and may act as a buffer against bladder wall irritants in patients with interstitial cystitis.²⁰ The characteristic macular abnormalities identified with multimodal retinal imaging, including multifocal hyperreflective lesions with cross-sectional and en face OCT and corresponding hyperautofluorescent lesions with FAF in the earlier stages of disease and frank retinal pigment epithelial atrophy including geographic atrophy and cRORA in the later stages, indicate that the retinal pigment epithelium may be a prime target of injury in patients with long-term PPS exposure. The reduction in choroidal stromal tissue detected in this study may indicate that the choroid could be an additional target of PPS toxicity, which may exacerbate retinal pigment epithelial disruption. However, it is also possible that choroidal impairment may be the secondary result of retinal pigment epithelial loss or vice versa. We acknowledge that it is also possible that the PPS-associated retinal pigment epithelial alterations may affect choroidal reflectivity and consequently the binarization and computation of CVI; therefore, our choroidal analysis awaits future validation with longitudinal studies. However, our results suggest that these choroidal metrics may prove to be additional surrogate markers of PPS toxicity that could be monitored by clinicians and retinal specialists.

PPS maculopathy is a very important masquerader of age-related macular degeneration (AMD), pattern, and mitochondrial dystrophies. Prior CVI analysis in eyes with drusen, geographic atrophy, and non-neovascular age-related macular degeneration have shown that both the SCA and CVI are decreased compared with non-AMD eyes.^{14,21-23} This is in contrast to the findings encountered in this study of eyes with PPS maculopathy. Recently, several studies using OCTA have demonstrated the importance of impaired choroidal vascular perfusion as a driving mechanism in the development and progression of atrophic AMD.^{24,25} Although AMD may be a vascular disease, PPS-associated maculopathy primarily may disrupt the epithelial and/or stromal tissues of the retina and choroid. More importantly, CVI may potentially provide an important tool to differentiate these overlapping diseases.

This cohort study is the largest prospectively performed screening analysis of a select cohort of participants with a history of PPS exposure using uniform and comprehensive multimodal retinal imaging, including SD-OCT, FAF, and NIR in all patients. However, the sample size of 100 represents a 13% participation rate out of 741 PPS-exposed subjects. Thus, the study's 16% prevalence of PPS-associated maculopathy may not be representative of the true prevalence within the general population of all PPS users at large. An overestimation due to ascertainment bias is possible. The mean duration of PPS use of screened patients in this study was 9.2 years. In comparison, a MarketScan database study revealed that only 130 (0.3%) of 49,899 patients diagnosed with interstitial cystitis had PPS prescriptions lasting longer than 5 years.²⁶ Although a significant proportion of our study subjects were asymptomatic, including several of the affected patients, those agreeing to participate may have been more likely to be symptomatic or informed of macular changes. Of note, this study's 13% participation rate is significantly lower than Vora and colleagues' screening rate of 85% (117 screened out of 138 PPS identified users).⁴ The prevalence of toxicity of 23.1% that Vora and colleagues reported may indicate that our prevalence is not an overestimation; however, their study only screened PPS patients with a cumulative exposure of at least 500 g. Future prospective studies with larger sample sizes will be necessary to determine the true prevalence of PPS maculopathy.

Limitations of this analysis include the lack of Early Treatment Diabetic Retinopathy Study (ETDRS) visual acuity testing and genetic analysis in all affected and indeterminate patients, including the indeterminate case with patternlike dystrophy findings. Case 100 underwent robust genetic analysis, but no mutation associated with patternlike dystrophy was identified. Genetic testing may prove useful in cases with abnormalities that can overlap with diseases such as pattern dystrophy and mitochondrial disorders. However, the unique phenotype of the disease combined with dosage guidelines and patient history should be sufficient for ophthalmologists to determine if genetic testing is warranted. Lastly, our total cohort of eyes used for the choroidal analysis was reduced as a result of exclusion of eyes with poor image quality and due to age-matching purposes.

This study continues to support the increasingly accepted concept that long-term PPS therapy can lead to symptomatic macular toxicity. Our prospectively performed screening protocol identified a 16% prevalence of maculopathy among patients with a history of PPS consumption who agreed to participate in the study, although the total cohort did include a significant proportion of long-term PPS users. All affected patients reported cumulative dosages greater than 1,500 g whereas 3 indeterminate cases including a case of patternlike dystrophy were associated with dosages greater than 1,000 g. Multimodal retinal imaging is critical for detection and diagnosis of the characteristic maculopathy, including FAF, NIR, and SD-OCT. NIR is

essential to detect the findings of mild PPS-associated maculopathy that include perifoveal hyperreflective dots. FAF is essential to detect the speckled pattern around the fovea and the disc, and peripapillary atrophy that was present in 100% of cases. FAF and SD-OCT are essential to detect the moderate and severe cases associated with pericentral and central geographic atrophy and cRORA. Ro-

bust choroidal analysis demonstrated increased CVI in PPS-affected patients compared with normal patients secondary to reduced SCA. Whether choroidal changes influence retinal pigment epithelial changes or vice versa in PPS patients is unclear but can be elucidated with continued research to better understand the mechanisms of PPS toxicity. CVI may provide a surrogate biomarker of macular toxicity.

ACKNOWLEDGMENTS AND DISCLOSURES

Funding/Support: This project was supported by the Research to Prevent Blindness Inc, New York, NY (David Sarraf), and the Macula Foundation Inc, New York, NY (David Sarraf). Financial Disclosures: Michael Ip receives consultancy fees from Boehringer Ingelheim, Thrombogenics, Quark, Omeros, Allergan, Amgen, Astellas, and Alimera and research support from Novartis, Genentech, Clearside, and Biogen. Srini Vas Satta receives consultancy fees from Amgen, Allergan, Bayer, Novartis, Genentech/Roche, Oxurion, Heidelberg Engineering, Optos, Carl Zeiss Meditec, and Centervue; financial support from Carl Zeiss Meditec; and nonfinancial support from Nidek and Topcon. David Sarraf receives consultancy fees from Amgen, Bayer, Genentech, and Optovue and research support from Genentech, Heidelberg, Optovue, Regeneron, and Topcon; is a speaker for Novartis; and provides expert professional services on behalf of plaintiffs in litigation related to Elmiron. The remaining authors have no financial disclosures.

All authors attest that they meet the current ICMJE criteria for authorship.

REFERENCES

1. Nickel JC, Moldwin R. FDA BRUDAC 2018 criteria for interstitial cystitis/bladder pain syndrome clinical trials: future direction for research. *J Urol*. 2018;200(1):39–42.
2. Pearce WA, Chen R, Jain N. Pigmentary maculopathy associated with chronic exposure to pentosan polysulfate sodium. *Ophthalmology*. 2018;125(11):1793–1802.
3. Wang D, Au A, Gunnemann F, et al. Pentosan-associated maculopathy: prevalence, screening guidelines, and spectrum of findings based on prospective multimodal analysis. *Can J Ophthalmol*. 2020;55(2):116–125.
4. Vora RA, Patel AP, Melles R. Prevalence of maculopathy associated with long-term pentosan polysulfate therapy. *Ophthalmology*. 2020;127(6):835–836.
5. Jain N, Li AL, Yu Y, VanderBeek BL. Association of macular disease with long-term use of pentosan polysulfate sodium: findings from a US cohort. *Br J Ophthalmol*. 2020;104(8):1093–1097.
6. Hanif AM, Armenti ST, Taylor SC, et al. Phenotypic spectrum of pentosan polysulfate sodium-associated maculopathy: a multicenter study. *JAMA Ophthalmol*. 2019;137(11):1275–1282.
7. Hanif AM, Shah R, Yan J, et al. Strength of association between pentosan polysulfate and a novel maculopathy. *Ophthalmology*. 2019;126(10):1464–1466.
8. Satta SR, Guymer R, Holz FG, et al. Consensus definition for atrophy associated with age-related macular degeneration on OCT: Classification of Atrophy report 3. *Ophthalmology*. 2018;125(4):537–548.
9. Guymer RH, Rosenfeld PJ, Curcio CA, et al. Incomplete retinal pigment epithelial and outer retinal atrophy in age-related macular degeneration: Classification of Atrophy Meeting report 4. *Ophthalmology*. 2020;127(3):394–409.
10. Fleckenstein M, Mitchell P, Freund KB, et al. The progression of geographic atrophy secondary to age-related macular degeneration. *Ophthalmology*. 2018;125(3):369–390.
11. Holz FG, Bellman C, Staudt S, Schütt F, Völcker HE. Fundus autofluorescence and development of geographic atrophy in age-related macular degeneration. *Invest Ophthalmol Vis Sci*. 2001;42(5):1051–1056.
12. Agrawal R, Chhablani J, Tan KA, Shah S, Sarvaiya C, Banker A. Choroidal vascularity index in central serous chorioretinopathy. *Retina*. 2016;36(9):1646–1651.
13. Vupparaboina KK, Nizampatnam S, Chhablani J, Richhariya A, Jana S. Automated estimation of choroidal thickness distribution and volume based on OCT images of posterior visual section. *Comput Med Imaging Graph*. 2015;46(pt 3):315–327.
14. Velaga SB, Nittala MG, Vupparaboina KK, et al. Choroidal vascularity index and choroidal thickness in eyes with reticular pseudodrusen. *Retina*. Apr 2020;40(4):612–617.
15. Vupparaboina KK, Dansingani KK, Goud A, et al. Quantitative shadow compensated optical coherence tomography of choroidal vasculature. *Sci Rep*. 2018;8(1):6461.
16. Nickel JC, Herschorn S, Whitmore KE, et al. Pentosan polysulfate sodium for treatment of interstitial cystitis/bladder pain syndrome: insights from a randomized, double-blind, placebo controlled study. *J Urol*. 2015;193(3):857–862.
17. Mishra K, Patel TP, Singh MS. Choroidal neovascularization associated with pentosan polysulfate toxicity. *Ophthalmol Retina*. 2020;4(1):111–113.
18. Satta SR. A path to the development of screening guidelines for pentosan maculopathy. *Can J Ophthalmol*. 2020;55(1):1–2.
19. Iovino C, Au A, Hilely A, et al. Evaluation of the choroid in eyes with retinitis pigmentosa and cystoid macular edema. *Invest Ophthalmol Vis Sci*. 2019;60(15):5000–5006.
20. Teichman JM. The role of pentosan polysulfate in treatment approaches for interstitial cystitis. *Rev Urol*. 2002;4(suppl 1):S21–S27.
21. Ozcaliskan S, Balci S, Yenerel NM. Choroidal vascularity index determined by binarization of enhanced depth imaging optical coherence tomography images in eyes with intermediate age-related macular degeneration. *Eur J Ophthalmol*. 2020;30(6):1512–1518.

22. Koh LHL, Agrawal R, Khandelwal N, Sai Charan L, Chhablani J. Choroidal vascular changes in age-related macular degeneration. *Acta Ophthalmol.* 2017;95(7):e597–e601.
23. Giannaccare G, Pellegrini M, Sebastiani S, et al. Choroidal vascularity index quantification in geographic atrophy using binarization of enhanced-depth imaging optical coherence tomographic scans. *Retina.* 2020;40(5):960–965.
24. Waheed NK, Moulton EM, Fujimoto JG, Rosenfeld PJ. Optical coherence tomography angiography of dry age-related macular degeneration. *Dev Ophthalmol.* 2016;56:91–100.
25. Borrelli E, Sarraf D, Freund KB, Sadda SR. OCT angiography and evaluation of the choroid and choroidal vascular disorders. *Prog Retin Eye Res* 11. 2018;67:30–55.
26. Ludwig CA, Vail D, Callaway NF, Pasricha MV, Moshfeghi DM. Pentosan polysulfate sodium exposure and drug-induced maculopathy in commercially insured patients in the United States. *Ophthalmology.* 2020;127(4):535–543.